OL Organic Letters

pubs.acs.org/OrgLett Letter

# 1,2-Hydroboration of Pyridines by Organomagnesium

Xinli Liu, Bingwen Li, Xiufang Hua, and Dongmei Cui*

Cite This: https://dx.doi.org/10.1021/acs.orglett.0c01388 Read Online

ACCESS | Metrics & More | Article Recommendations | Supporting Information

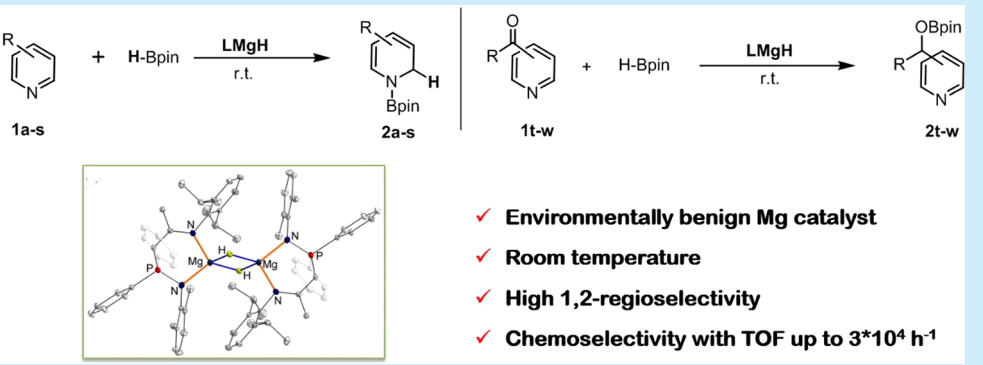


**ABSTRACT:** Hydroboration of pyridine derivatives at room temperature with earth-abundant and biocompatible magnesium catalysts ligated by phosphinimino amides is developed. Fine turnover frequency (TOF) and distinguished 1,2-regioselectivity have been achieved. The exclusive chemoselective carbonyl hydroboration happens with competitive TOF. A HBpin assisted mechanism is deduced by the reaction rate law, activation parameters, and kinetic isotope effect (KIE) in combination with DFT calculations. To our knowledge, this is the first example of pyridine 1,2-dearomatization by Mg-based catalysts.

Downloaded via UNIV OF NEW ENGLAND on June 13, 2020 at 13:41:08 (UTC).
See https://pubs.acs.org/sharingguidelines for options on how to legitimately share published articles.

Dihydropyridine derivatives are important intermediates for preparing organic compounds, biologically active agents, and medicines. For constructing the dihydropyridine skeletons, reduction of pyridines by mild reducing reagents such as silanes and boranes instead of highly flammable $H_2$ gas, has been accepted as a convenient method recently.[1] Thus, designing catalysts to collaborate with these reagents and to hydrogenate in regioselective manner become the research focus. The first catalytic hydroboration of pyridines by using the $\beta$-diketiminate ligated magnesium complex gives a mixture of 1,2- and 1,4-regioselective products.[2] Interestingly, recently prosperous Lewis acid units and some ruthenium based catalyst have shown high 1,4-selectivity (Figure 1).[3,4] Comparatively, synthesis of 1,2-dihydropyridines, the important intermediates in the preparation of nitrogenous natural products and drug targets,[5,6] has encountered several obstacles: low reaction efficiency, harsh conditions, or using precious or poisonous metal-based catalysts.[7] Important advances have been obtained recently by the innovation of lanthanide and iron complexes.[5,8] With respect to the earth-abundant and biobenign alkaline earth metals, research progress is much slower. Only a few calcium based complexes show major 1,2-regioselectivity under harsh conditions, which is often accompanied by loss of activity due to the Schlenk-type ligand redistribution.[9] Some magnesium complexes can react stoichiometrically with pyridine to afford a 1,2-dihydropyridine adduct, but they are almost inert toward catalytic pyridine dearomatization under ambient temperature. In addition, the

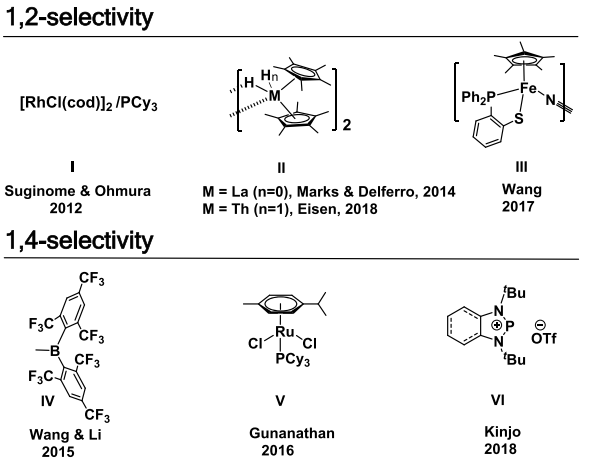


**Figure 1.** Representative catalysts for high 1,2- and 1,4-selective hydroboration of pyridines.

**Received:** April 22, 2020


© XXXX American Chemical Society

https://dx.doi.org/10.1021/acs.orglett.0c01388
Org. Lett. XXXX, XXX, XXX−XXX

transformed thermodynamic 1,4-product was obtained when the reaction was heated.[2,10] Thus, for magnesium based complexes, accelerating the kinetic 1,2-selective reaction and preventing the thermodynamic 1,4-reaction/transformation, become the key issue for obtaining high 1,2-dihydropyridine product.

Herein, we developed magnesium complexes ligated by phosphinimino amides (Scheme 1). Complexes **1** ($R^1$ = Cy (cyclohexyl)) was previously reported by our group and complex **2** ($R^1$ = Ph) was synthesized with similar method.[11] Dinuclear complexes **1** and **2** bridging by two hydrides were defined by NMR spectrum analyses and characterized with X-ray diffraction analyses (For the crystal structures of complexes **1** and **2**: hydrogen atoms (except the Mg−H) are omitted for clarity. Thermal ellipsoids are drawn at the 20% probability level).

**Scheme 1. Structures of Phosphinimino-amido Magnesium Complexes 1 and 2**

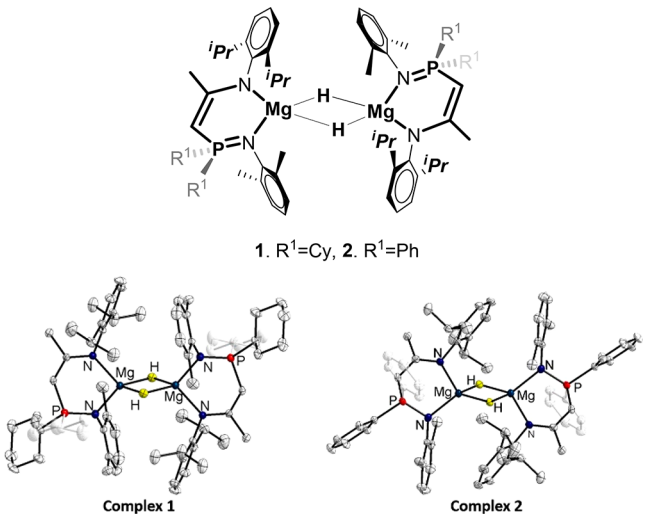


At room temperature, **1** was relatively inert to HBpin but quickly reacted with pyridine to yield complex **4** containing two pyridine moieties: one is 1,2-reduced pyridine via Mg−H transfer, and the other is a coordinated neutral pyridine (Figures S1, S61−S63).[12]

After mixing HBpin, pyridine, and catalyst **1** together, no signal was seen for complex **4** but a major 1,2-hydroboration product appeared in NMR monitoring spectra (Figures S64−S67). The catalytic reaction proceeded smoothly to reach complete conversion within 10 h at a ratio of *N*-Bpin-1,2-dihydropyridine (**2a**)/*N*-Bpin-1,4-dihydropyridine (**2a′**) > 20:1. To our delight, the TOF enhanced correspondingly from 12.1 $h^{-1}$ to 134.5 $h^{-1}$ when the reaction temperature increased from 25 to 70 °C, while the product ratio of **2a**:**2a′** remained unchanged (Table 1, entries 1−3 and Table S2). Complex **2** bearing the ligand with $R^1$ = Ph displayed analogous catalytic activity and 1,2-regioselectivity at either room temperature or high temperature (Table 1, entries 5 and 6). On the other hand, a polar solvent like THF decreases the **2a**:**2a**′ ratio down to 1.3:1, which should be derived from the competitive coordination of THF (Table 1, entry 4). On the other hand, *β*-diketiminate skeleton ligated magnesium hydride complex **3** was inert to the reaction at room temperature but afforded a mixture at high temperature (Table 1, entry 7).[1,2] To our knowledge, complexes **1** and **2** are the first magnesium-based catalysts to reach high 1,2-regioselective dearomatization of pyridine, especially in a wide temperature scope.

**Table 1. Hydroboration of Pyridine Catalyzed by 1−3**

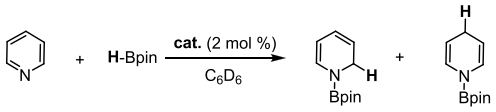


1a 2a 2a'

| entry[a] | cat | *T* (°C) | time (h) | yield (%) | (**2a**:**2a′**)[b] |
|---|---|---|---|---|---|
| 1 | **1** | 25 | 10 | 99.5 | >20:1 |
| 2 | **1** | 40 | 1 | 98.3 | >20:1 |
| 3 | **1** | 70 | 0.2 | 99.2 | >20:1 |
| 4[c] | **1** | 25 | 30 | 71.4 | 1.3:1 |
| 5 | **2** | 25 | 10 | 99.0 | >20:1 |
| 6 | **2** | 70 | 0.2 | 99.1 | >20:1 |
| 7 | **3**[d] | 70 | 20 | 64.0 | 1.9:1 |

[a]Reaction conditions: pyridine (0.20 mmol), HBpin (0.20 mmol), $C_6D_6$ as solvent (0.50 mL). Catalyst loading is 2 mol % relative to pyridine. [b]Yields and **2a**:**2a′** ratio were determined by $^1$H NMR spectroscopy using methyltriphenylsilane as an internal standard. [c]$C_4D_8O$ ($d_8$-THF) as a solvent. [d]**3** is magnesium hydride complex ligated with *β*-diketiminate skeleton.[12c]

The following investigations on various pyridine reagents were then carried out with **1**, and the collected data are listed in Scheme 2 and Table S2. Under mild conditions, para-substituted pyridines were exclusively transformed to 1,2-products (**2b**, **2c**). For pyridines with meta-substituents like methyl, methoxyl, and halogens, the 1,2-selective products *N*-boryl-3-substituted-1,2-dihydropyridines (**2d**−**2j**) were predominant regardless of the substituent type. The electron-withdrawing group accelerated the reaction, as the adjacent carbon was easily attacked by a nucleophilic species. Contrarily, the electron-donating group retarded the reaction since it made the reduction of the adjacent carbon very difficult. Thus, the TOF value for the dearomatization of the pyridines varied with the electronics of the meta-substituent, following the trend of I > Br > Cl > *F* > Ph> Me > OMe (Table S2). On the other hand, the different trend of them on 1,2-selectivity was presumably due to steric encumbrance. Much stronger electron withdrawing nitro and cyano groups led to some side-reaction with the catalyst instead of the regular hydroboration reaction.[4c] When using 2-methyl-pyridine, 2,2-bipyridyl, and 2-methyl-quinoline as the reagents, no dearomatization took place even at elevated temperatures, as the *ortho*-block in pyridines significantly impedes the dearomatization process.[4,5] The mostly active reactions were found for quinolines and isoquinolines (TOF > 1500 $h^{-1}$), and the 1,2-selective products of **2k** and **2l** were exclusively isolated, which might be attributed to the less aromatic stabilization of them. Thus, even with a methyl substituent such as 3-methyl-quinoline, 3-methyl-isoquinoline, and even 1-methyl-isoquinoline, the reactions proceeded smoothly to give pure 1,2-regioselective products **2m**, **2n**, and **2o**. With regard to the *N*-heterocylcles like pyrazine, pyrimidine, 2,5-dimethyl-pyrazine, and quinoxaline, 2 equiv of HBpin was required to produce the doubly hydroborated products **2p**, **2q**, **2r**, and **2s** in good yields.

The extremely high activity and excellent chemoselective reduction on the carbonyl substituent rather than the pyridine ring were realized when using the carbonyl substituted pyridines (Scheme 3). For example, quantitative conversion of 2-acetyl-pyridine to **2t** was finished in less than 2 min with 1


https://dx.doi.org/10.1021/acs.orglett.0c01388
Org. Lett. XXXX, XXX, XXX−XXX

**Scheme 2. 1,2-Hydroboration of Pyridines Catalyzed by 1**[a]

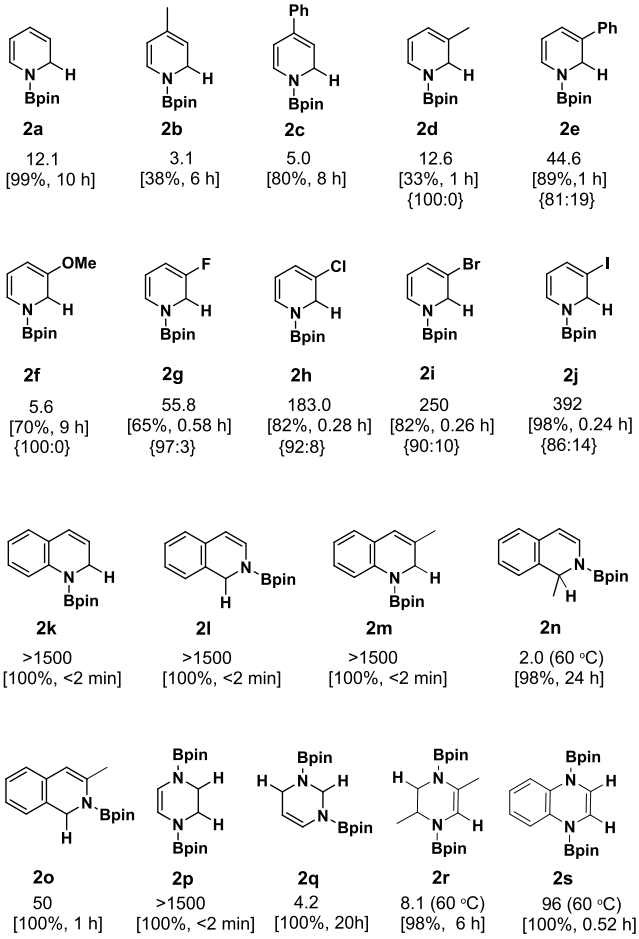


[a]Reaction conditions: Pyridine (0.189 mmol), HBpin (0.189 mmol), cat = complex **1** ($3.77 \times 10^{-3}$ mmol), and $Ph_3SiMe$ ($20 \times 10^{-3}$ mmol) in 0.5 mL $C_6D_6$ at 25 °C. Turnover frequencies (TOF = [product] [catalyst]$^{-1}$ $h^{-1}$) by $^1H$ NMR analysis with $Ph_3SiMe$ internal standard.[4] Quantities in brackets are NMR yields and corresponding reaction times. Isomer ratios in braces refer to ratios of regioisomeric 3- and 5-substituted-1,2-dihydropyridines.

**Scheme 3. Chemoselective Hydroboration of Carbonyl Substituted Pyridines**[a]

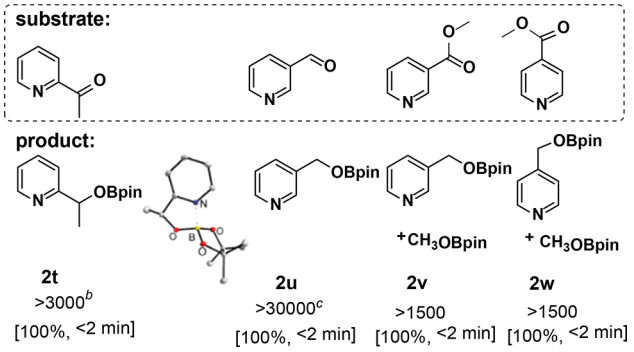


[a]Reaction conditions: Pyridine (0.189 mmol), HBpin (0.189 mmol), cat = complex **1** ($3.77 \times 10^{-3}$ mmol), $Ph_3SiMe$ ($20 \times 10^{-3}$ mmol) in 0.5 mL $C_6D_6$ at 25 °C. [b][cat] = 1 mol %. [c][cat] = 0.1 mol %.

mol % catalyst loading,[13] while only 0.1 mol % catalyst was needed to quantitatively converse 3-aldehyde-pyridine to **2u** with a recorded high TOF of $3 \times 10^4$ $h^{-1}$. For methyl ester substituted pyridines, the equivalent boroxane substituted pyridines (**2v** and **2w**) and $CH_3OBpin$ were achieved.

Kinetic rate law of the reaction was calculated according to the ln−ln plots of different $[\mathbf{1}]_0$ vs initial rate ($\nu_i$), which is the first order dependence on [Mg]. Fixing the catalyst concentration as constant, the first-order dependence on [HBpin] as well as the second-order dependence on [pyridine] are determined (eq 1 and Figure 2a−c). An inverse

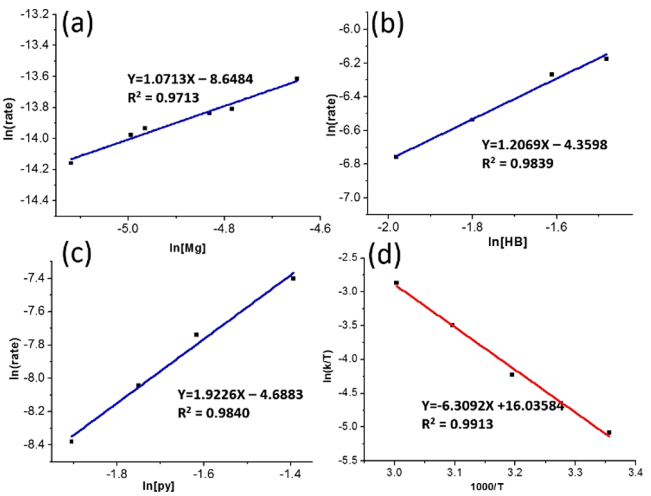


**Figure 2.** Ln−ln plot of the different $[\text{substrate}]_0$ vs corresponding initial rate: (a) $\ln[Mg]_0/\ln(\text{rate})$, (b) $\ln[HBpin]_0/\ln(\text{rate})$, and (c) $\ln[\text{pyridine}]_0/\ln(\text{rate})$. (d) Eyring plot with the line as the least-squares fit to the data points.

dependence on [heterocycle] or [HBpin] was previously reported, respectively, in which a pre-equilibrium between the active species and inactive heterocycle composing intermediate (or inactive HBpin composing intermediate) were presumed.[5,14] $^1H$ NMR spectra of the reaction under various temperatures ranging from 298 to 333 K gave activation parameters calculated according to the standard Eyring equation: $\Delta H^{\ddagger}$ = 12.5 kcal mol$^{-1}$, $\Delta S^{\ddagger}$ = −15.34 cal mol$^{-1}$, and $E_a$ = 13.1 kcal mol$^{-1}$ (Figure 2d). The large negative $\Delta S^{\ddagger}$ suggests organized transition state characteristics as in the earlier reports for such reactions.[15]

$$\frac{d[P]}{dt} = k_{obs}[Mg]^1[\text{pyridine}]^2[HBpin]^1 \quad (1)$$

Furthermore, a H/D kinetic isotope effect (KIE) experiment was applied for detecting the rate-determining step. As compared to the different initial reaction rates of the **1**/HBpin/py system and **1**/DBpin/py system with identical conditions, a high H/D KIE of 3.93 was obtained (Figures S68−S69 and Table S3). Combined with the first order of HBpin in rate law (1), the B−H bond cleavage step is confirmed as the rate-determining process. This result further implies that the pyridine dearomatization process overcomes a lower activation energy than that of the B−H bond cleavage process. The easier dearomatization step may explain the high 1,2-regioselectivity in our system, as the 1,2-selective product is the result of kinetics control.

DFT calculations were further employed to investigate the 1,2-regioselective mechanism based on our system.[16−19] As shown in Scheme 4, upon coordinating with 1 equiv of Py, complex **1** (precat) is hypothesized to cleave into the monomeric INT1 by breaking the H-bridge with a smaller


https://dx.doi.org/10.1021/acs.orglett.0c01388
Org. Lett. XXXX, XXX, XXX−XXX

**Scheme 4. DFT-Derived Energy Profiles of 1,2- vs 1,4-Regioselective Pathways**

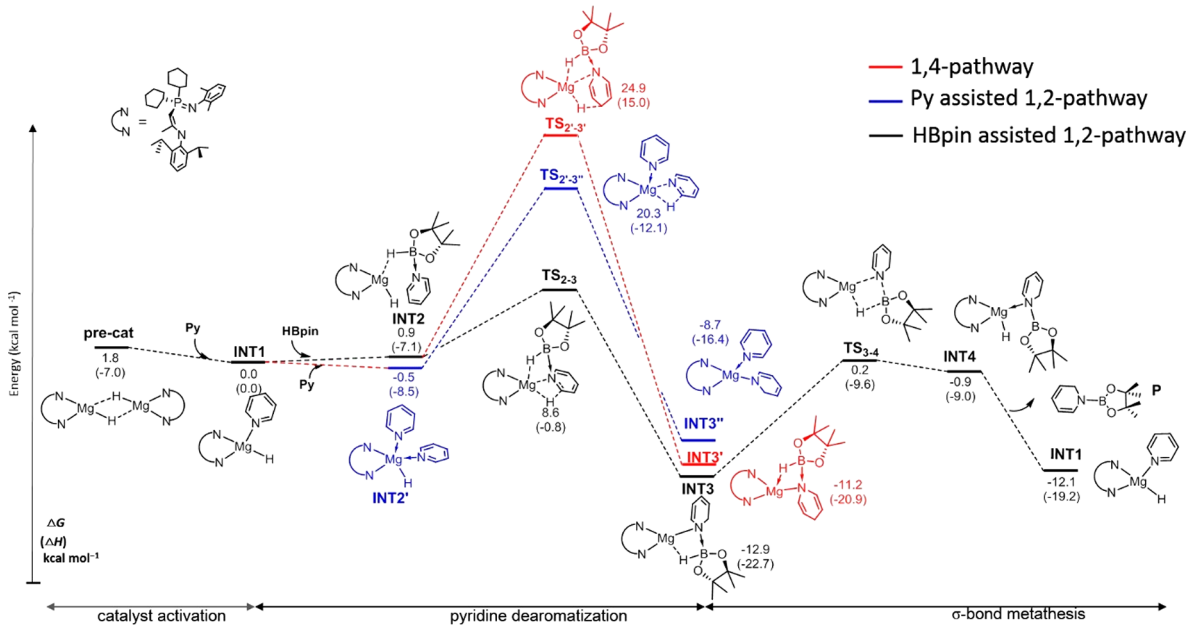


$\Delta G$ of −1.8 kcal/mol. INT1 is artificially set as the active species since it is more stable than precat. INT2 was formed from INT1 after adding a HBpin molecule (black line) or alternatively adding another Py (INT2′) (blue line) with a similar energy barrier (−0.5 vs 0.9 kcal/mol). The sharp difference of activation energy during the following 1,2-dearomatization of Mg−H to Py was observed that only 7.7 kcal/mol was needed for HBpin coordinated/assisted $TS_{2-3}$ than 20.8 kcal/mol for Py assisted $TS_{2'-3''}$. The high energy of 24 kcal/mol for 1,4-dearomatization process through $TS_{2'-3'}$ made 1,4-pathway very difficult (red line). INT3 contains a dearomatized Py ligand and a HBpin, which via Mg−N/H−B metathesis reaction gives the intermediate INT4 in terms of the putative four-centered transition state of $TS_{3-4}$. INT4 releases P to recover the active species INT1, which is a spontaneous process. In addition, the activation enthalpy $\Delta H$ of 13.1 kcal $mol^{-1}$ in $TS_{3-4}$ is comparable with the corresponding $\Delta H^{\ddagger}$ of 12.5 kcal $mol^{-1}$ calculated by the Eyring equation within their error margins (Figure 2d). The slightly higher energy barrier for the formation of INT4 (13.1 kcal/mol) than intermediate INT3 (7.7 kcal/mol) clearly indicates that the cleavage of the B−H bond is the rate-limiting step, which is in accordance with experimental results.[5] Moreover, HBpin plays a crucial role in reducing the activation energy of the pyridine dearomatization process as well as stabilizing the following intermediate INT3. As a result, the kinetically and thermodynamically feasible 1,2-dearomatization pathway is accomplished in our system.

In summary, the hydroboration of various pyridines by using the magnesium complexes with excellent regio- and chemoselectivity has been achieved. From the reagent viewpoint, the electron-withdrawing group on pyridines and *N*-heterocycles without a steric block like quinoline, isoqunoline, 3-methylquinoline, and pyrazine accelerates the reaction rate. DFT simulation reveals that HBpin is involved in the reaction circle at the pyridine dearomatization step, in which 1,2-dearomatization is the obvious preferred process and the intermediate of 1,2-DHP is more stable than that of 1,4-DHP. The following Mg−N/H−B metathesis reaction is the turnover-determining step due to the larger activation energy, which is in agreement with the kinetics studies. This research demonstrates that divalent magnesium based complexes are promising catalysts for high regioselective hydroboration of pyridines.

## ■ ASSOCIATED CONTENT

### Supporting Information

The Supporting Information is available free of charge at https://pubs.acs.org/doi/10.1021/acs.orglett.0c01388.

Experimental section and computational details (PDF)

### Accession Codes

CCDC 1868409 and 1890791 contain the supplementary crystallographic data for this paper. These data can be obtained free of charge via www.ccdc.cam.ac.uk/data_request/cif, or by emailing data_request@ccdc.cam.ac.uk, or by contacting The Cambridge Crystallographic Data Centre, 12 Union Road, Cambridge CB2 1EZ, UK; fax: +44 1223 336033.

## ■ AUTHOR INFORMATION


### Corresponding Author

**Dongmei Cui** − *State Key Laboratory of Polymer Physics and Chemistry, Changchun Institute of Applied Chemistry, Chinese Academy of Sciences, Changchun 130022, China; University of Chinese Academy of Sciences, Changchun 130022, China;* orcid.org/0000-0001-8372-5987; Email: dmcui@ciac.ac.cn

### Authors

**Xinli Liu** − *State Key Laboratory of Polymer Physics and Chemistry, Changchun Institute of Applied Chemistry, Chinese Academy of Sciences, Changchun 130022, China*

**Bingwen Li** − *Laboratory of Theoretical and Computational Chemistry, Institute of Theoretical Chemistry, Jilin University, Changchun 130023, China*

**Xiufang Hua** − *State Key Laboratory of Polymer Physics and Chemistry, Changchun Institute of Applied Chemistry, Chinese*




https://dx.doi.org/10.1021/acs.orglett.0c01388
Org. Lett. XXXX, XXX, XXX−XXX

*Academy of Sciences, Changchun 130022, China*

Complete contact information is available at: https://pubs.acs.org/10.1021/acs.orglett.0c01388

## Author Contributions

All authors have given approval to the final version of the manuscript.

## Notes

The authors declare no competing financial interest.

## ■ ACKNOWLEDGMENTS

We are grateful to the financial supports from the National Natural Science Foundation of China for project Nos. 21774119, 21574125.

## ■ REFERENCES

(1) (a) Chatterjee, B.; Gunanathan, C. Catalytic Dearomative Hydroboration of Heteroaromatic Compounds. *J. Chem. Sci.* **2019**, *131* (12), 118. (b) Bull, J. A.; Mousseau, J. J.; Pelletier, G.; Charette, A. B. Synthesis of Pyridine and Dihydropyridine Derivatives by Regio- and Stereoselective Addition to *N*-Activated Pyridines. *Chem. Rev.* **2012**, *112*, 2642−2713. (c) Park, K. Recent Advances in Catalytic Dearomative Hydroboration of N-Heteroarnes. *ChemCatChem* **2020**, DOI: 10.1002/cctc.201902303.

(2) (a) Arrowsmith, M.; Hill, M. S.; Hadlington, T.; Kociok-Koehn, G.; Weetman, C. Magnesium-Catalyzed Hydroboration of Pyridines. *Organometallics* **2011**, *30*, 5556−5559. (b) Chong, C. C.; Kinjo, R. Catalytic Hydroboration of Carbonyl Derivatives, Imines, and Carbon Dioxide. *ACS Catal.* **2015**, *5*, 3238−3259. (c) Rochat, R.; Lopez, M. J.; Tsurugi, H.; Mashima, K. Recent Developments in Homogeneous Organomagnesium Catalysis. *ChemCatChem* **2016**, *8*, 10−20.

(3) (a) Kaithal, A.; Chatterjee, B.; Gunanathan, C. Ruthenium-Catalyzed Regioselective 1,4-Hydroboration of Pyridines. *Org. Lett.* **2016**, *18*, 3402−3405. (b) Tamang, S. R.; Singh, A.; Unruh, D. K.; Findlater, M. Nickel-Catalyzed Regioselective 1,4-Hydroboration of N-Heteroarenes. *ACS Catal.* **2018**, *8*, 6186−6191.

(4) (a) Fan, X.; Zheng, J.; Li, Z. H.; Wang, H. Organoborane Catalyzed Regioselective 1,4-Hydroboration of Pyridines. *J. Am. Chem. Soc.* **2015**, *137*, 4916−4919. (b) Keyzer, E. N.; Kang, S. S.; Hanf, S.; Wright, D. S. Regioselective 1,4-hydroboration of pyridines catalyzed by an acid-initiated boroniumcation. *Chem. Commun.* **2017**, *53*, 9434−9437. (c) Rao, B.; Chong, C. C.; Kinjo, R. Metal-Free Regio- and Chemoselective Hydroboration of Pyridines Catalyzed by 1,3,2-Diazaphosphenium Triflate. *J. Am. Chem. Soc.* **2018**, *140*, 652−656.

(5) Dudnik, A. S.; Weidner, V. L.; Motta, A.; Delferro, M.; Marks, T. J. Atom-efficient regioselective 1,2-dearomatization of functionalized pyridines by an earth-abundant organolanthanide catalyst. *Nat. Chem.* **2014**, *6*, 1100−1107.

(6) (a) Oshima, K.; Ohmura, T.; Suginome, M. Regioselective Synthesis of 1,2-Dihydropyridines by Rhodium-Catalyzed Hydroboration of Pyridines. *J. Am. Chem. Soc.* **2012**, *134*, 3699−3702. (b) Pang, M. F.; Chen, J. Y.; Zhang, S. J.; Liao, R. Z.; Tung, C. H.; Wang, W. G. Controlled Partial Transfer Hydrogenation of Quinolines by Cobalt-Amido Cooperative Catalysis. *Nat. Commun.* **2020**, *11*, 1249−1258.

(7) Park, S.; Chang, S. Catalytic Dearomatization of *N*-Heteroarenes with Silicon and Boron Compounds. *Angew. Chem., Int. Ed.* **2017**, *56*, 7720−7738.

(8) (a) Zhang, F.; Song, H.; Zhuang, X.; Tung, C.-H.; Wang, W. Iron-Catalyzed 1,2-Selective Hydroboration of *N*-Heteroarenes. *J. Am. Chem. Soc.* **2017**, *139*, 17775−17778. (b) Liu, H.; Khononov, M.; Eisen, M. S. Catalytic 1,2-Regioselective Dearomatization of *N*-Heteroaromatics via a Hydroboration. *ACS Catal.* **2018**, *8*, 3673−3677. (c) Bullock, R. M. Abundant Metals Give Precious Hydrogenation Performance. *Science* **2013**, *342*, 1054−1055. (d) Liu, T. W.; He, J. H.; Zhang, Y. T. Regioselective 1,2-Hydroboration of N-Heteroarenes using a Potassium-based Catalyst. *Org. Chem. Front.* **2019**, *6*, 2749−2756.

(9) Intemann, J.; Bauer, H.; Pahl, J.; Maron, L.; Harder, S. Calcium Hydride Catalyzed Highly 1,2-Selective Pyridine Hydrosilylation. *Chem. - Eur. J.* **2015**, *21*, 11452−11461.

(10) (a) Intemann, J.; Lutz, M.; Harder, S. Multinuclear Magnesium Hydride Clusters: Selective Reduction and Catalytic Hydroboration of Pyridines. *Organometallics* **2014**, *33*, 5722−5729. (b) Mukherjee, D.; Shirase, S.; Spaniol, T. P.; Mashima, K.; Okuda, J. Magnesium hydridotriphenylborate $[Mg(thf)_6][HBPh_3]_2$: a versatile hydroboration catalyst. *Chem. Commun.* **2016**, *52*, 13155−13158. (c) Rauch, M.; Ruccolo, S.; Parkin, G. Synthesis, Structure, and Reactivity of a Terminal Magnesium Hydride Compound with a Carbatrane Motif, $[Tism^{PriBenz}]MgH$: A Multifunctional Catalyst for Hydrosilylation and Hydroboration. *J. Am. Chem. Soc.* **2017**, *139*, 13264−13267. (d) Fohlmeister, L.; Stasch, A. Ring-Shaped Phosphinoamido-Magnesium-Hydride Complexes: Syntheses, Structures, Reactivity, and Catalysis. *Chem. - Eur. J.* **2016**, *22*, 10235−10246. (e) Lemmerz, L. E.; Spaniol, T. P.; Okuda, J. 1,4-Dihydropyridyl complexes of magnesium: synthesis by pyridine insertion into the magnesium-silicon bond of triphenylsilyls and catalytic pyridine hydrofunctionalization. *Dalton Trans* **2018**, *47*, 12553−12561.

(11) (a) Xie, H.; Liu, X.; Cui, D. Regioselective Ring Opening Reactions of Pyridine *N*-Oxide Analogues by Magnesium Hydride Complexes. *Organometallics* **2017**, *36*, 3597−3604. (b) Xie, H.; Hua, X.; Liu, B.; Wu, C.; Cui, D. Phosphinimino-amino supported complex: Synthesis, polymerization of ethylene and dearomatisation of pyridine. *J. Organomet. Chem.* **2015**, *798*, 335−340.

(12) Mixed compounds of 1,2-dihydropyridide anion and 1,4-dihydropyridide containing Mg complexes were reported when *β*-diketiminato-supported *n*-butyl magnesium complex reacted with $PhSiH_3$ and following pyridine. See (a) Hill, M. S.; MacDougall, D. J.; Mahon, M. Magnesium Hydride-promoted Dearomatisation of Pyridine. *Dalton, Trans* **2010**, *39*, 11129−11131. (b) Hill, M. S.; Kociok-Kohn, G.; MacDougall, D. J.; Mahon, M. F.; Weetman, G. Magnesium Hydrides and the Dearomatisation of Pyridine and Quinoline. *Dalton, Trans* **2011**, *40*, 12500−12509. (c) See the Supporting Information for the detailed structure and synthesis route of complex **3**.

(13) (a) Weidner, V. L.; Barger, C. J.; Delferro, M.; Lohr, T. L.; Marks, T. J. Rapid, Mild, and Selective Ketone and Aldehyde Hydroboration/Reduction Mediated by a Simple Lanthanide Catalyst. *ACS Catal.* **2017**, *7*, 1244−1247. (b) Arrowsmith, M.; Hadlington, T. J.; Hill, M. S.; Kociok-Kohn, G. Magnesium-catalyzed Hydroboration of Aldehydes and Ketones. *Chem. Commun.* **2012**, *48*, 4567−4569. (c) The X-ray structure of **2t** was previously reported by Y. Lebedev (Y. Lebedev, 2019. CSD Communication (Private Communication)) with CCDC number of 1888986.

(14) Weetman, C.; Hill, M. S.; Mahon, M. F. Magnesium-catalysed Hydroboration of Pyridines: Kinetic Analysis and Poly-pyridine Dearomatisation. *Polyhedron* **2016**, *103*, 115−120.

(15) Gutsulyak, D. V.; van der Est, A.; Nikonov, G. I. Facile Catalytic Hydrosilylation of Pyridines. *Angew. Chem., Int. Ed.* **2011**, *50*, 1384−1387.

(16) Molecular geometries of all complexes are optimized at the M06-2X level of density functional theory. The 6-31g (d,p) basis set are used for all atoms like Mg, B, P, C, O, N, and H. Frequency calculations at the same level of theory are also performed to identify all the stationary points as minima (zero imaginary frequencies) or transition states (one imaginary frequency) and to provide the thermal correction to free energies at 298.15 K and 1 atm. Zhao, Y.; Truhlar, D. G. The M06 suite of density functionals for main group thermochemistry, thermochemical kinetics, noncovalent interactions, excited states, and transition elements: two new functionals and systematic testing of four M06-class functionals and 12 other functionals. *Theor. Chem. Acc.* **2008**, *120*, 215−241.

(17) (a) Zhao, Y.; Truhlar, D. G. Benchmark Energetic Data in a Model System for Grubbs II Metathesis Catalysis and Their Use for

the Development, Assessment, and Validation of Electronic Structure Methods. *J. Chem. Theory Comput.* **2009**, *5*, 324−333. (b) Zhao, Y.; Truhlar, D. G. Density functionals with broad applicability in chemistry. *Acc. Chem. Res.* **2008**, *41*, 157−167.

(18) Hariharan, Pc; Pople, J. A. Influence of polarization Functions on Molecular-orbital Hydrogenation Energies. *Theor. Chim. Acta* **1973**, *28*, 213−222.

(19) The similar multihydrogen bridged structure of $\mathbf{TS_{2-3}}$ is also observed in the intermediates using magnesium or calcium catalyst. See (a) Harvey, M. J.; Hanusa, T. P.; Pink, M. Unusual stability of the coordinated triethylborohydride anion in an alkaline-earth metal complex: crystallographic characterization of $Ca(HBEt_3)\{1,2,4\text{-}C_5(SiMe_3)_3H_2\}(thf)_2$. *Chem. Commun.* **2000**, 489−490. (b) Mukherjee, D.; Ellern, A.; Sadow, A. D. Magnesium-catalyzed hydroboration of esters: evidence for a new zwitterionic mechanism. *Chem. Sci.* **2014**, *5*, 959−964. (c) Also the model of Mg-O-B bridge" based transition state is excluded as depicted in Schemes S2 and S3.



https://dx.doi.org/10.1021/acs.orglett.0c01388
*Org. Lett.* XXXX, XXX, XXX−XXX